Silence Analysis of AMPA Receptor Mutated at the CaM-Kinase II Phosphorylation Site

Victor A. Derkach
Vollum Institute, Oregon Health Sciences University, Portland, Oregon 97201

ABSTRACT Direct phosphorylation of the GluR1 subunit of postsynaptic AMPA receptors by Ca^{2+}/calmodulin-dependent protein kinase II (CaM-KII) is believed to be one of the major contributors to the enhanced strength of glutamatergic synapses in CA1 area of hippocampus during long-term potentiation. The molecular mechanism of AMPA receptor regulation by CaM-KII is examined here by a novel approach, silence analysis, which is independent of previously used variance analysis. I show that three fundamental channel properties—single-channel conductance, channel open probability, and the number of functional channels—can be measured in an alternative way, by analyzing the probability of channels to be simultaneously closed (silent). Validity of the approach was confirmed by modeling, and silence analysis was applied then to the GluR1 AMPA receptor mutated at S831, the site phosphorylated by CaM-KII during long-term potentiation. Silence analysis indicates that a negative charge at S831 is a critical determinant for the enhanced channel function as a charge carrier. Silence and variance analyses, when applied to the same sets of data, were in agreement on the receptor regulation upon mutations. These results provide independent evidences for the mechanism of AMPA receptor regulation by CaM-KII and further strengthens the idea how calcium-dependent phosphorylation of AMPA receptors can contribute to the plasticity at central glutamatergic synapses.

INTRODUCTION

Modulation of properties of ion channels in the plasma membrane is a common molecular mechanism for altering physiological responses. This is especially true for single-channel conductance, open probability, and the number of functional channels, inasmuch as their product ultimately links channel behavior to the macroscopic membrane conductance. Two approaches have been broadly employed for measuring these fundamental channel properties: variance (originally called noise analysis, Katz and Miledi, 1970; Sigworth, 1980, Traynelis et al., 1993) and single-channel analyses (Hamill et al., 1981; Colquhoun and Hawkes, 1995; Colquhoun and Sigworth, 1995). These insightful approaches have, however, some limitations. Reliable determination of the number of functional channels by variance analysis is critically dependent on a high open probability of the channels involved. This condition dictates high or saturating agonist concentrations, if ligand-gated ion channels are of interest. In contrast, correct measurements of single-channel currents require recordings from either one functional channel (this might be difficult to prove; see Horn, 1991; also see Colquhoun and Hawkes, 1995) or from a population of channels with a low open probability, to observe well-separated single-channel events. The latter is usually accomplished by using low agonist concentrations. However, determination of the number of functional channels becomes challenging at low open probability (Horn, 1991; Colquhoun and Hawkes, 1995), and channel properties can also depend on the concentration of agonist used, if the property is a function of receptor occupancy by agonist (Rosenmund et al., 1998; Smith et al., 2000; Smith and Howe, 2000). Thus, variance and singe-channel analyses may not necessarily speak for the same values because of different experimental requirements. Therefore, it would be beneficial to develop techniques that measure channel properties under the same experimental conditions as, for example, variance analysis does, but independently. This would allow a cross-examination of a particular molecular mechanism by such techniques, and thus a firm establishment of the mechanism.

Here I propose such an approach, silence analysis, and apply it to an important problem of modern neuroscience—the regulation of AMPA-type glutamate receptors by CaM-KII. This kinase is crucial for the enhanced strength of glutamate synapses during long-term potentiation (LTP; see Malinow et al., 1989; Silva et al., 1992; Giese et al., 1998), a cellular model for memory and learning. The activity of CaM-KII increases upon induction of LTP (Fukunaga et al., 1993, Barria et al., 1997a) and one of major substrates for this kinase in the postsynaptic density is the GluR1 subunit of AMPA receptors (McGlade-McCulloh et al., 1993; Barria et al., 1997a; Lee et al., 2000; Yoshimura et al., 2000) phosphorylated at Ser831 on the C-terminus. (Barria et al., 1997b; Mammen et al., 1997; Lee et al., 2000; Huang et al., 2001). This phosphorylation results in increased channel conductance of GluR1 AMPA receptor (Derkach et al., 1999), and is reminiscent of the increased conductance of postsynaptic AMPA receptors during LTP (Benke et al., 1998) or upon elevation of CaM-KII activity in CA1 pyramidal neurons (Poncer et al., 2002). These data on the regulation of AMPA receptors by CaM-KII have been previously obtained through variance and single-channel analyses, which were performed, however, under different

Submitted June 13, 2002, and accepted for publication November 7, 2002.

Address reprint requests to Victor A. Derkach, Vollum Institute L-474, Oregon Health Sciences University, 3181 S.W. Sam Jackson Park Rd., Portland, OR 97201. Tel.: 503-494-6904, Fax: 503-494-4534, E-mail: derkachv@ohsu.edu.

0006-3495/03/03/1701/08 $2.00

experimental conditions. In the present study, the receptor regulation is tested independently and nonambiguously: by applying silence analysis to the GluR1 AMPA receptor mutated at the CaM-KII site, and by concurrent application of silence and variance analyses to the same sets of data.

METHODS

Electrophysiology

Experiments where performed on HEK-293 cells expressing the flip version of the GluR1 AMPA receptor subunit. Transfection and recording conditions were as described earlier (Derkach et al., 1999). All recordings were performed in outside-out patches. Patch pipettes were filled with the following solution (in mM): 160 CsCl, 2 $MgCl_2$, 4 Na-ATP, 1 EGTA, 10 HEPES, pH 7.3. Extracellular solution contained (in mM): 165 NaCl, 2.5 KCl, 1 $MgCl_2$, 2 $CaCl_2$, 5 HEPES, pH 7.3. Fast application of glutamate to outside-out patches was performed by piezo-driven application system or by puffing. Glutamate at 10 mM was applied in pulses of 40–50 ms with 5-s intervals between pulses. Currents were recorded at room temperature and membrane potentials −80 mV to −140 mV using an Axopatch 1B amplifier (Axon Instruments, Union City, CA). Frequency bandwidth and sampling rate were 1–2 kHz and 5–10 kHz, respectively (pCLAMP6 software, Axon Instruments). Statistics on channel parameters are presented as mean ± SE. Difference in values of a parameter was considered significant if $p < 0.05$, as evaluated by two-tailed Student's *t*-test.

Analyses

A total of 37–99 trials were performed on individual patches to collect data for concurrent application of silence or nonstationary variance analyses. For both techniques, experimental data were fitted by theoretical functions using Chi-square minimization procedure (KaleidaGraph, Synergy Software, Reading, PA). The relationship between the variance, *var*, of macroscopic current fluctuations and the mean current, *I*, was fitted by the function (Sigworth, 1980),

$$\mathrm{var} = iI - I^2/N + \mathrm{var_b}, \quad (1)$$

where two unknowns, i (single-channel current) and N (number of functional channels), were free parameters, and var_b was the variance of background noise. Open probability P_o was calculated at the peak of the mean current using equation

$$P_o = I/iN. \quad (2)$$

Single-channel chord conductance was calculated as

$$\gamma = i/(V_m - V_o), \quad (3)$$

where V_m and V_0 are membrane potential and reversal potential, respectively.

For silence analysis (described in the text, Fig. 1), the threshold for detection of single-channel openings was set at 3σ of background noise to minimize its contribution to the estimated silence factor. The actual contribution of false events related to the noise was measured in the absence of glutamate applications using deflections of noise opposite in polarity to the channel activity. It was less than 1% of the total number of detected events, and its contribution to the silent factor was regarded as negligible.

Simulations

Channel activity was simulated using a cyclic model of the AMPA receptor (Partin et al., 1996; Banke et al., 2000; see also Fig. 2 *A*) and Axograph 4.2 software (Axon Instruments). The model was run at 10 kHz sampling and filtration bandwidth 2 kHz resembling our experimental conditions. Parameters of the model were adjusted to reproduce properties of the flip version of GluR1 receptor, because this receptor was examined in our experiments

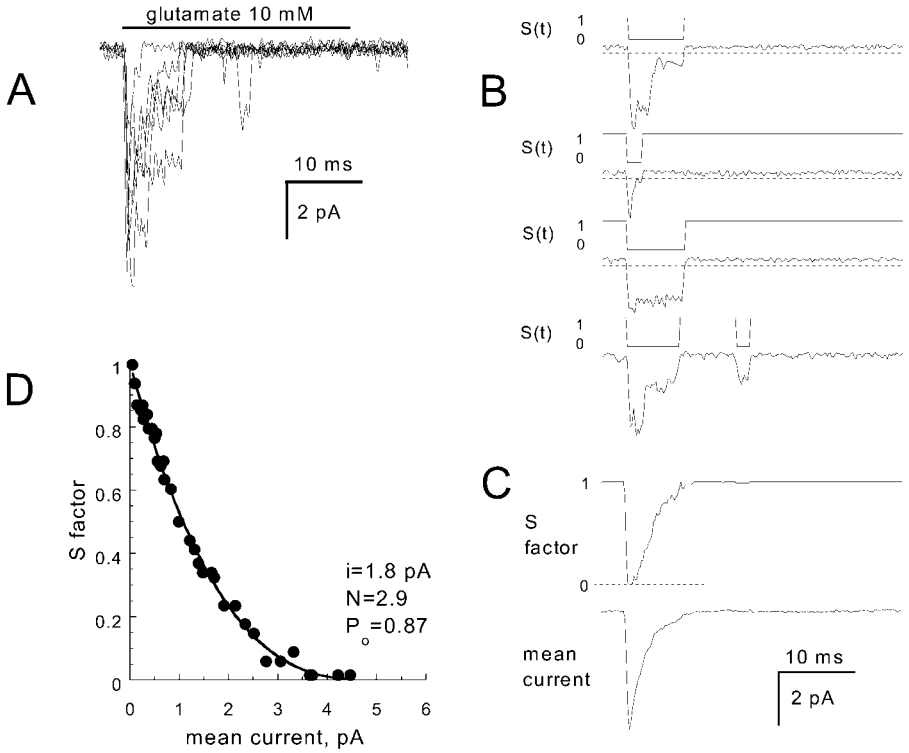

FIGURE 1 Silence analysis of D831 mutant of GluR1 receptor. (*A*) Currents evoked by pulses of 10 mM glutamate in an outside-out patch from a cell expressing the D831 mutant of GluR1 receptor (membrane potential −100 mV). Seven traces are shown. (*B*) Measuring the silence factor $S(t)$ as a binary function of time for some of trials shown in *A*. In each pair of traces, a top trace is $S(t)$ versus the corresponding trial (*bottom trace*). The dotted line is the threshold for detection of channel openings/closings. (*C*) The averaged *S* factor (*top*) and the averaged macroscopic current (*bottom*) from 84 trials, some of which are shown in *B*. (*D*) *S* factor as a function of the mean current was fitted by Eq. 6 (*solid line*) with i and N as free parameters. The peak open probability, P_o, was calculated as $P_o = I_p/(i \times N)$, where I_p is a peak current.

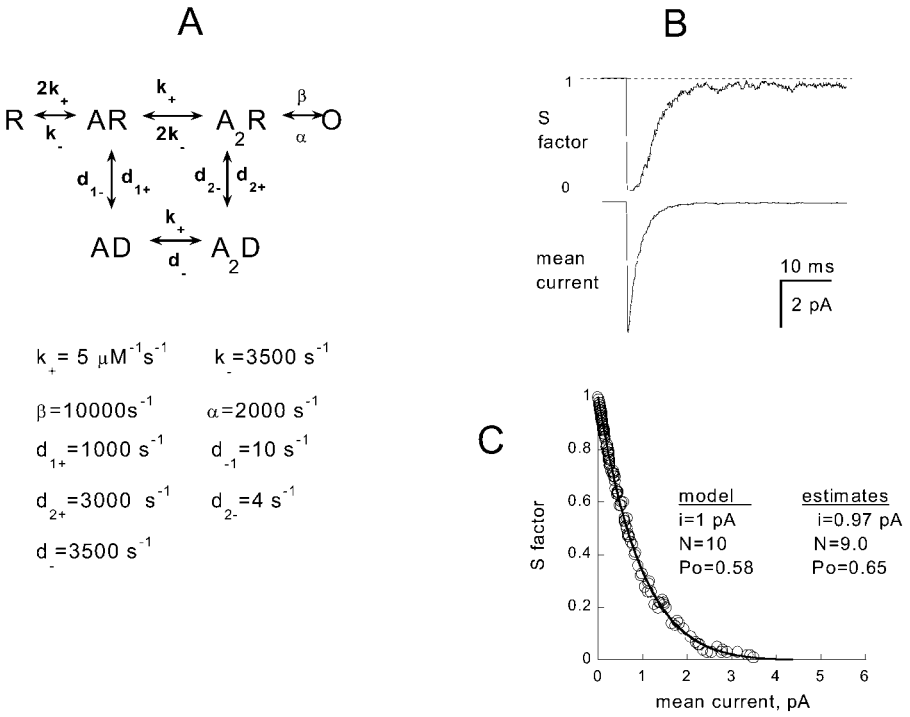

FIGURE 2 Validity of silence analysis. (*A*) Kinetic model for the flip version of GluR1 AMPA receptor used for simulations. All states except *O* (*open channel*) represent a receptor with a closed channel. ''*A*'' denotes an agonist; *AR* and A_2R are agonist-receptor complexes with one and two bound molecules of agonist, respectively. *AD* and A_2D indicate desensitized receptor. (*B*) Silence factor (*top trace*) and macroscopic current from a set of 100 trials generated by the model for conditions shown in *C*. (*C*) Determination of channels parameters from the data shown in *B*. Channel parameters were calculated as explained in Fig. 1. Note a close match between model parameters and estimates.

(Mosbacher et al., 1994; Partin et al., 1996; Derkach et al., 1999; Banke et al., 2000); including: activation and inactivation kinetics, kinetics of desensitization and recovery, steady-state desensitization, agonist dependence of desensitization kinetics, apparent affinity to glutamate, and the peak open probability of channels (Table 1). The model was run then in a stochastic mode. Conditions of low (0.128) and high (0.58) open probabilities were achieved at 0.3 mM and 10 mM glutamate, respectively. For each set of channel parameters, 100 trials were collected for a single analysis (run), and 16–20 of such runs were generated for each set of experimental conditions to verify accuracy and stability of the analysis. Estimates of each parameter are presented as mean ± SE (Fig. 3) and the accuracy of the analyses was evaluated by an estimation error calculated as a relative deviation of estimated parameter from its model value. Because in a real experiment the threshold for detection of channel openings/closings can vary in regard to the amplitude of single-channel currents, silence analysis was performed at different thresholds of detection for each run (set at 0.2, 0.5, and 0.8 of single-channel current amplitude and shown by different symbols on Fig. 3) and for every set of experimental conditions, to see how this may affect the analysis outcome.

TABLE 1 Properties of GluR1 (flip) AMPA receptor and its model (Fig. 2 *A*)

Property	Model	GluRi	References
Activation time, $t_{10–90}$ (ms)	0.3	0.3–0.4	(*3*, *4*)
Deactivation, τ, ms (1 ms glutamate pulse):			
Glutamate 1 mM	1.02	0.79	(*1*)
Glutamate 10 mM	1.01	0.9	(*4*)
Desensitization, τ_{des}, ms	2.36	2.1–2.5	(*1–3*)
Steady-state desensitization, %	1.1	1–2	(*3*, *4*)
Recovery from desensitization, τ_{rec}, ms	120	100–150	(*1*, *2*)
EC_{50}, mM (peak current)	0.86	0.75	(*2*)
Hill coefficient	1.29	1.1	(*2*)
Peak open probability	0.58	0.55–0.75	(*2*, *3*)

All kinetic parameters of $GluR1_i$ are given for outside-out patches at 10 mM glutamate and at –60 mV to –80 mV of membrane potential. Note a close match between predictions of the model and the real receptor. References are: (*1*) Partin et al., 1996; (*2*) Derkach et al., 1999; (*3*) Banke et al., 2000; and (*4*) Derkach, unpublished.

RESULTS

Channel silence carries information on channel properties: silence analysis

If channels are functionally identical and independent (as variance analysis also assumes) and adopt two states (open and closed), their activity can be defined as a binominal process. In a population of N channels the probability to find m channels open simultaneously, $P_{o,m}$, is

$$P_{o,m} = \frac{N!}{m!(N-m)!} P_o^m (1-P_o)^{N-m}, \quad (4)$$

where P_o is the probability of a channel to be open. Using this equation for measuring the number of channels in a population is notoriously challenging, especially at low P_o (Horn, 1991; Colquhoun and Hawkes, 1995). The problem is that channel openings are not explicit on the actual number of channels (N) contributing to the activity. Another approach would be to look at the closed states of the channels. Indeed, at moments of time when channels are simultaneously closed their contributing number becomes explicit and should be identified as ''all channels.'' These moments in channel activity can be directly measured and treated quantitatively as a probability for all channels being

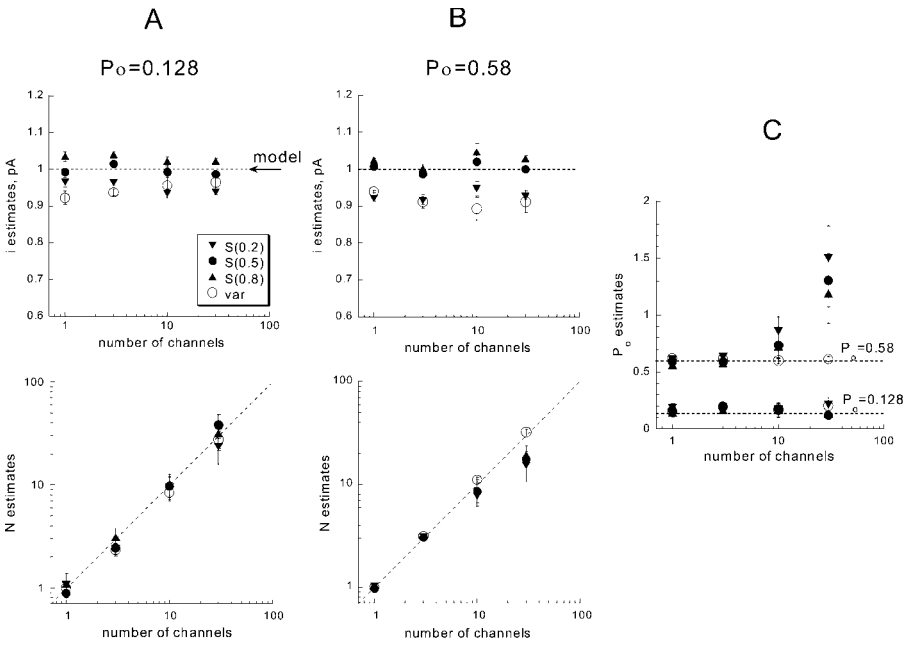

FIGURE 3 Performance of silence analysis under different experimental conditions. (*A* and *B*) Estimations of single-channel current (*top panels*) and the number of functional channels (*bottom*) under low (*A*) and high (*B*) open probabilities. Different closed symbols represent different levels of the threshold for detection of channel openings and closings in regard to the amplitude of single-channel current (see Experimental Procedures). Open circles represent estimates of variance analysis. (*C*) Estimations of open probability as a function of the number of functional channels and channel open probability. Dashed lines in all panels represent corresponding model values. Note that the analysis predicts closely all channel parameters when P_o is low, and performs well even at high P_o if the number of channels in a population is small (fewer than 10).

simultaneously silent (closed), or a silent factor *S*. This factor is an extreme condition for the above equation when $m = 0$, so as

$$S = P_{o,m}|_{m=0} = (1 - P_o)^N. \quad (5)$$

This equation can be also expressed as a function of macroscopic current *I* after substitution for P_o from Eq. 2:

$$S = (1 - I/(iN))^N \quad (6)$$

Two channel parameters, *i* and *N*, can be found then upon fitting *S* values by Eq. 6, and P_o can be calculated using Eq. 2. Note, the initial slope of *S* factor carries information on single-channel current.

$$\lim_{I \to 0}\left(\frac{dS}{dI}\right) = -\left(\frac{1}{i}\right)\lim_{I \to 0}\left(1 - \frac{I}{iN}\right)^{N-1} = -\frac{1}{i}. \quad (7)$$

Critically, Eq. 6 cannot be obtained by a combination of Eqs. 1 and 2, indicating silence analysis is independent of variance analysis.

Measuring *S* factor and channel parameters

For a population of channels, their probability to be simultaneously silent at a particular moment of time was calculated as a relative frequency of finding all of the channels closed. An example of calculations of *S* factor for actual channel activity is shown on Fig. 1. Activity of GluR1 AMPA receptors was evoked in an outside-out patch by repetitive applications of 10 mM glutamate (Fig. 1 *A*). In each trial, for those periods of time when all channels were simultaneously closed (no events above the threshold of detection), the value of $S(t)$ was assigned 1 (successful event) and 0 otherwise (failure) (Fig. 1 *B*, *upper traces* in each pair). *S* factor was calculated then as a weighted value of $S(t)$, upon averaging of $S(t)$ for each time point across multiple trials (Fig. 1 *C*, *upper trace*). Channel properties were found upon fitting the relationship between *S* factor and the macroscopic current by Eq. 6 with *i* and *N* as free parameters (Fig. 1 *D*, *solid line*). P_o was calculated then from Eq. 2.

Thus, all three values, *i*, *N*, and P_o can be determined without knowledge of the power of fluctuations of macroscopic current, which would be required for variance analysis. That suggests silence analysis as a new and alternative tool for evaluation of channel properties.

Accuracy and limitations

Due to its nature, silence analysis puts certain requirements on the experimental situation. The approach assumes *S* factor is a measurable value, and that requires that during a macroscopic response all channels in a population will be temporary and simultaneously closed. As Eq. 5 states, such events in channel activity can be infrequent, if either the open probability or the number of functional channels is high. This may affect the accuracy of the silence factor calculations and thus measurements of channel parameters. Therefore, I tested silence analysis in more detail, under variable and controllable conditions provided by modeling experiments (Figs. 2 and 3, see Experimental Procedures). I was particularly interested to see how well the approach performs at low versus high open probability and with a variable number of channels in a population. Deviation of each estimated parameter from its modeling value was calculated as an estimation error. The method was particularly precise in

measuring single-channel current (the error was between 1% and 8%) independently of experimental conditions (Fig. 3, *A* and *B*). Calculations of N and P_o were also close to the model (the error ranged from 1% to 28%) as long as open probability was low or channel population was small (10 channels or below, Fig. 3, *A–C*). However, for a high open probability (0.6) and increased population of channels (more than 10), the error became significant (49% for N and 125–170% for P_o, Fig. 3, *B* and *C*).

Overall, the approach was quite sensitive for the evaluation of channel conductance in a broad range of conditions, being more accurate and persistent than nonstationary variance analysis at low P_o and small channel population (Fig. 3). It was also reliable for measuring of N and P_o, if the number of channels in a population was small (~10 or less); whereas variance analysis became more accurate at a high P_o and bigger channel population (Fig. 3). Therefore, to measure all three properties using both approaches simultaneously, I followed the requirement of small channel population by restricting the number of channels in my patch experiments to fewer than 10–12. This reduced the number of suitable patches to 13 from the total of 49 analyzed.

Testing S831 mutants

I chose two mutants of the GluR1 receptor with either aspartate or alanine at position S831, the residue phosphorylated by CaM-KII during LTP in the CA1 region of hippocampus (Barria et al., 1997a; Lee et al., 2000; Huang et al., 2001). These mutations functionally mimic the receptor either phosphorylated by CaM-KII or dephosphorylated at S831, respectively (Barria et al., 1997b; Mammen et al., 1997; Derkach et al., 1999) and maximized the functional homogeneity of the receptor population in regard to the phosphorylation state of S831.

Silence analysis applied to the D831 mutant (Fig. 1 and Fig. 4 *A*) revealed that the single-channel conductance ranged from 20 pS to 31.8 pS, having an average value of 24.3 ± 1.4 pS ($n = 7$, Fig. 4 *A*). In contrast, single-channel conductance of the A831 mutant was significantly lower, having an average value of 12.8 ± 0.8 pS ($p < 0.01$, variations from 8.9 pS to 15.3 pS, Fig. 4 *A*). Channel open probabilities varied broadly for both mutants (Fig. 4 *B*), from 0.36 to 0.87 for the S831D mutant with an average value of 0.55 ± 0.07 ($n = 7$; coefficient of variation, $CV = 0.31$), and from 0.35 to 0.71 for the S831A mutant, with an average value of 0.54 ± 0.06 ($n = 6$, $CV = 0.28$, Fig. 4 *B*) and were not distinguishable ($p = 0.42$).

Silence and variance analyses agree on AMPA receptor regulation

Using two independent approaches, under the same experimental conditions, provided the opportunity of scrutinizing AMPA receptor regulation through their cross-examination. I therefore concurrently applied variance analysis to those individual patches where silence analysis was also performed. Example of such concurrent analyses is shown in Fig. 5. When variance analysis was applied (Fig. 5, *A* and *B*) to the same data previously analyzed by silence analysis (Fig. 1), their estimates were closely matched (Fig. 5 *C*). When all patches were analyzed in the same manner, both approaches confirmed a lower single-channel conductance of the A831 mutant (Fig. 6 *A*, *left*). Variance analysis gave single-channel conductance of 12.5 ± 1.2 pS ($n = 6$) compared to 12.8 ± 0.8 pS by silence analysis for the A831 mutant, and of 25.1 ± 1.6 pS ($n = 7$) and 24.3 ± 1.4 pS, respectively, for the D831 mutant (Fig. 6 *A*, *right*). Both techniques were also in agreement on channel open probability in individual patches (Fig. 6 *B*, *left*), as variance analysis gave 0.48 ± 0.05 ($n = 6$, $CV = 0.26$) compared to

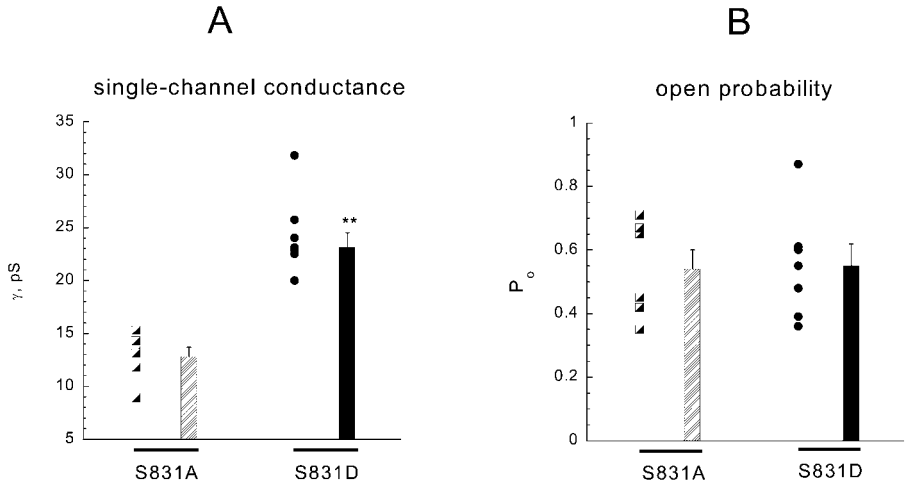

FIGURE 4 Silence analysis indicate increased channel conductance for the S831D mutant of GluR1 AMPA receptor. (*A*) Estimates of single-channel conductance provide lower values for the S831A ($n = 6$) than for the S831D mutant ($n = 7$). Each point represents a particular patch and bars are means ± SE. In contrast to channel conductance, channel open probability (*B*) was not distinguishable between mutants. ** indicates $p < 0.01$.

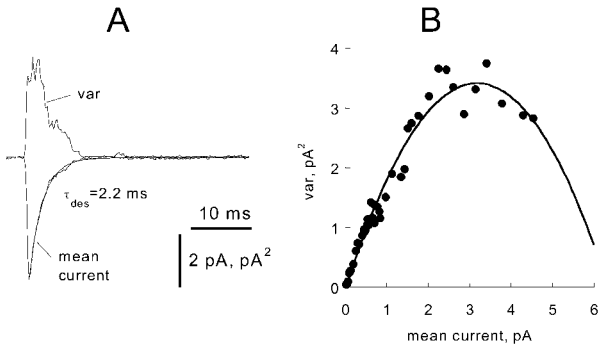

C

	silence analysis	variance analysis
i, pA	1.8	2.1
P_o	0.87	0.74
N	2.9	2.9

FIGURE 5 Comparison of variance and silence analyses for the same channel activity. (*A*) Variance (*upper trace*) and mean current for the patch from Fig. 1 *A*. (*B*) Nonstationary variance analysis for the data in *A*. Fitting (*solid curve*) was performed as described in the Methods. (*C*) Estimates of channel properties provided by silence and variance analyses when both were applied to the same channel activity (shown in Fig. 1 *A*). Note a close match between these two independent approaches.

0.54 ± 0.06 ($CV = 0.28$) by silence analysis for the A831 mutant, and 0.50 ± 0.05 ($n = 7$, $CV = 0.26$) and 0.55 ± 0.07 ($CV = 0.31$), respectively, for the D831 mutant (Fig. 6 *B*, *right*). The agreement between the two approaches was also confirmed by a tight correlation of estimates for γ, P_o, and N, as correlation coefficients were 0.92, 0.88, and 0.95 for γ, P_o, and N, respectively (Fig. 6). Ratios of values estimated by silence analysis to those by variance analysis were 1.01 ± 0.04, 0.96 ± 0.1 and 1.07 ± 0.04 for γ, P_o, and N, respectively ($n = 13$ for each parameter).

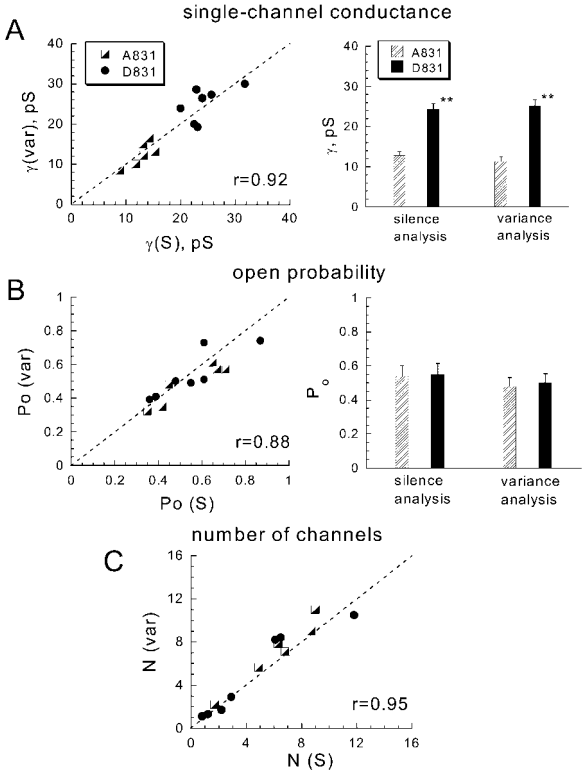

FIGURE 6 Agreement between silence and variance analyses on properties of GluR1 receptor mutants. Single-channel conductance (*A*, *left*), open probability (*B*, *left*) and number of functional channels (*C*) determined by both methods in the same patches for D831 ($n = 7$, *circles*) and A831 ($n = 6$, *squares*) mutants of GluR1 receptor. Parameters calculated by silence and variance analyses are denoted by *S* and *var*, respectively. Note, all points are close to the dotted lines with a slope 1 representing ''the line of agreement'' when both approaches give identical measurements. Values estimated by both techniques highly correlated as indicated by coefficients of correlation, *r*. The right panels in *A* and *B* represent average values for γ and P_o obtained by both techniques (from data on the left). Essential, higher channel conductance for the D831 mutant is detected by both approaches. ** indicates $p < 0.01$.

DISCUSSION

Silence analysis: perspectives

This study illustrates the utility of silence analysis as an alternative approach to investigate molecular mechanisms of membrane conductances. This method brings several opportunities to the field. First, it provides a new and independent way for estimating the three principal channel parameters, single-channel current, channel open probability, and the number of functional channels. Second, it is possible now to apply two alternative techniques (silence and variance analyses) in the same experimental situation. This gives an opportunity of rigorously testing a particular hypothesis through their cross-examination. Thirdly, silence analysis provides a third independent equation (Eq. 6) to the system of two (Eqs. 1 and 2). In principal, each channel parameter, *i*, *N*, and P_o, can now be found independently of each other on the basis of three experimental values: *I*, *var*, and *S*. Therefore, a direct link between a particular channel property and the macroscopic membrane conductance can be investigated.

Although the present study demonstrates an application of silence analysis to nonstationary channel activity, there are no principal limitations to use it in equilibrium, for steady-state channel activity. The universal requirement would be the same—small channel population.

AMPA receptor regulation by CaM-KII

This study presents new evidences for the mechanism of AMPA receptor regulation by CaM-KII. First, silence analysis independently shows that a negative charge at S831 of GluR1 receptor is critical for the enhanced efficiency of channel as a charge carrier, because of increased channel conductance. Second, the mechanism was scrutinized by simultaneous application of silence and variance analyses

to the same sets of data. This eliminates the ambiguity of different experimental conditions previously used for variance and single-channel analyses to examine the regulation of the GluR1 AMPA receptor by CaM-KII (Derkach et al., 1999). Because both approaches agree on the mechanism, this further strengthens the conclusion of how the AMPA receptor is regulated by CaM-KII mediated phosphorylation.

Results of this study strongly support the recent finding on the regulation of postsynaptic AMPA receptors by CaM-KII. Overexpression of constitutively active form of the kinase in CA1 pyramidal neurons of hippocampus resulted in increased single-channel conductance of synaptic AMPA receptors (assayed by variance analysis) to be apparently a major contributing mechanism to the enhanced synaptic strength, and this was accompanied by increased phosphorylation of the S831 (Poncer et al., 2002). These observations are consistent with the increased channel conductance of synaptic AMPA receptors during LTP expression (Benke et al., 1998; Luthi et al., 1999). Silence analysis provides new and independent evidences for the molecular mechanism of AMPA receptor regulation by CaM-KII, and further strengthens the idea of how calcium-dependent phosphorylation of AMPA receptors can contribute to the plasticity at central glutamatergic synapses (Lisman et al., 1997; Malenka and Nicoll, 1999; Soderling and Derkach, 2000).

AMPA channel multiconductance and synaptic strength

It becomes increasingly apparent that AMPA receptors can adopt multiple conductance states. This is true for native (Jahr and Stevens, 1987; Cull-Candy and Usowicz, 1987; Banke et al., 2000; Smith et al., 2000; Smith and Howe, 2000) and recombinant receptors (Swanson et al., 1997; Rosenmund et al., 1998; Derkach et al., 1999; Banke et al., 2000). The functional significance for such channel multiconductance was unclear until recently. It was found that 1), LTP in the CA1 region of hippocampus is accompanied by an increased conductance of postsynaptic AMPA receptors in the majority of potentiated synapses (Benke et al., 1998); and 2), the conductance of AMPA receptors can be increased by increasing the contribution of high conductance states to the channel activity. The latter can be achieved in two different ways, however—either by increasing the receptor occupancy by agonist (Rosenmund et al., 1998; Smith et al., 2000; Smith and Howe, 2000) or through receptor phosphorylation by CaM-KII (Derkach et al., 1999, this study). These observations bring in focus two critical questions: whether postsynaptic AMPA receptors in CA1 synapses are saturated upon glutamate release (reviewed in Bergles et al., 1999; Clements, 1996; see also Liu et al., 1999; McAllister and Stevens, 2000) and what is the phosphorylation status of postsynaptic AMPA receptors before and after LTP induction (reviewed in Swope et al., 1999; Soderling and Derkach, 2000; see also Lee et al., 2000; Huang et al., 2001). Although other mechanisms for the regulation of synaptic strength should be also considered (Malinow et al., 2000; Luscher et al., 1999; Sheng and Lee, 2001; Huber et al., 2000; Liu and Cull-Candy, 2000; Linden, 2001), the data presently collected in the field strongly indicate that the increase in AMPA receptor conductance mediated by CaM-KII is one of the major contributors to LTP in CA1 hippocampal synapses (Lisman et al., 1997; Malenka and Nicoll, 1999; Lisman et al., 2002; Poncer et al., 2002). Interestingly, this regulation of synaptic strength is specific for a particular form of plasticity because AMPA receptors are selectively phosphorylated at S831 during LTP but dephosphorylated at S845 during LTD (Lee et al., 2000; Huang et al., 2001) and this is accompanied by increased channel conductance during LTP (Benke et al., 1998), but not LTD (Luthi et al., 1999). One remaining question is, what is the relative contribution of the modified channel properties versus incorporation of new receptors for the enhanced synaptic strength?

In memory of dear friend and brilliant neuroscientist Alexander Selyanko (1952–2001).

I thank Drs. Craig Jahr, Jeff Diamond, Matt Jones, Laurence Trussell, Thomas Soderling, and Coleen Atkins for insightful discussions and critical reading.

This work has been supported by a grant from the Medical Research Foundation.

REFERENCES

Banke, T. G., D. Bowie, H. Lee, R. L. Huganir, A. Schousboe, and S. F. Traynelis. 2000. Control of GluR1 AMPA receptor function by cAMP-dependent protein kinase. *J. Neurosci.* 20:89–102.

Barria, A., D. Muller, V. Derkach, L. C. Griffith, and T. R. Soderling. 1997a. Regulatory phosphorylation of AMPA-type glutamate receptors by CaM-KII during long-term potentiation. *Science*. 276:2042–2045.

Barria, A., V. Derkach, and T. R. Soderling. 1997b. Identification of the Ca2+/calmodulin-dependent protein kinase II regulatory phosphorylation site in the alpha-amino-3-hydroxyl-5-methyl-4-isoxazole-propionate-type glutamate receptor. *J. Biol. Chem.* 272:32727–32730.

Benke, T. A., A. Luthi, J. T. Isaac, and G. L. Collingridge. 1998. Modulation of AMPA receptor unitary conductance by synaptic activity. *Nature*. 393:793–797.

Bergles, D. E., J. S. Diamond, and C. E. Jahr. 1999. Clearance of glutamate inside the synapse and beyond. *Curr. Opin. Neurobiol.* 9:293–298.

Clements, J. D. 1996. Transmitter time course in the synaptic cleft: its role in central synaptic function. *Trends Neurosci.* 19:163–171.

Colquhoun, D., and A. G. Hawkes. 1995. The principles of the stochastic interpretation of ion-channel mechanisms. *In* Single-Channel Recordings. B. Sakmann, and E. Neher, editors. Plenum, New York. pp397–482.

Colquhoun, D., and F. J. Sigworth. 1995. Fitting and statistical analysis of single-channel records. *In* Single-Channel Recordings. B. Sakmann, and E. Neher, editors. Plenum, New York. pp483–587.

Cull-Candy, S. G., and M. M. Usowicz. 1987. Multiple-conductance channels activated by excitatory amino acids in cerebellar neurons. *Nature*. 325:525–528.

Derkach, V., A. Barria, and T. R. Soderling. 1999. Ca2+/calmodulin-KII enhances channel conductance of alpha-amino-3-hydroxy-5-methyl-4-

isoxazolepropionate type glutamate receptors. *Proc. Natl. Acad. Sci. USA*. 96:3269–3274.

Fukunaga, K., L. Stoppini, E. Miyamoto, and D. Muller. 1993. Long-term potentiation is associated with an increased activity of Ca2+/calmodulin-dependent protein kinase II. *J. Biol. Chem*. 268:7863–7867.

Giese, K. P., N. B. Fedorov, R. K. Filipkowski, and A. J. Silva. 1998. Autophosphorylation at Thr286 of the alpha calcium-calmodulin kinase II in LTP and learning. *Science*. 279:870–873.

Hamill, O. P., A. Marty, E. Neher, B. Sakmann, and F. J. Sigworth. 1981. Improved patch-clamp techniques for high-resolution current recording from cells and cell-free membrane patches. *Pflugers Arch*. 391:85–100.

Horn, R. 1991. Estimating the number of channels in patch recordings. *Biophys. J*. 60:433–439.

Huang, C. C., Y. C. Liang, and K. S. Hsu. 2001. Characterization of the mechanism underlying the reversal of long term potentiation by low frequency stimulation at hippocampal CA1 synapses. *J. Biol. Chem*. 276:48108–48117.

Huber, K. M., M. S. Kayser, and M. F. Bear. 2000. Role for rapid dendritic protein synthesis in hippocampal mGluR-dependent long-term depression. *Science*. 288:1254–1257.

Jahr, C. E., and C. F. Stevens. 1987. Glutamate activates multiple single channel conductances in hippocampal neurons. *Nature*. 325:522–525.

Katz, B., and R. Miledi. 1970. Membrane noise produced by acetylcholine. *Nature*. 226:962–963.

Lee, H. K., M. Barbarosie, K. Kameyama, M. F. Bear, and R. L. Huganir. 2000. Regulation of distinct AMPA receptor phosphorylation sites during bidirectional synaptic plasticity. *Nature*. 405:955–959.

Linden, D. J. 2001. The expression of cerebellar LTD in culture is not associated with changes in AMPA- receptor kinetics, agonist affinity, or unitary conductance. *Proc. Natl. Acad. Sci. USA*. 98:14066–14071.

Lisman, J., R. C. Malenka, R. A. Nicoll, and R. Malinow. 1997. Learning mechanisms: the case for CaM-KII. *Science*. 276:2001–2002.

Lisman, J., H. Schulman, and H. Cline. 2002. The molecular basis of CaMKII function in synaptic and behavioral memory. *Nat. Rev. Neurosci*. 3:175–190.

Liu, G., S. Choi, and R. W. Tsien. 1999. Variability of neurotransmitter concentration and nonsaturation of postsynaptic AMPA receptors at synapses in hippocampal cultures and slices. *Neuron*. 22:395–409.

Liu, S. Q., and S. G. Cull-Candy. 2000. Synaptic activity at calcium-permeable AMPA receptors induces a switch in receptor subtype. *Nature*. 405:454–458.

Luscher, C., H. Xia, E. C. Beattie, R. C. Carroll, M. von Zastrow, R. C. Malenka, and R. A. Nicoll. 1999. Role of AMPA receptor cycling in synaptic transmission and plasticity. *Neuron*. 24:649–658.

Luthi, A., R. Chittajallu, F. Duprat, M. J. Palmer, T. A. Benke, F. L. Kidd, J. M. Henley, J. T. Isaac, and G. L. Collingridge. 1999. Hippocampal LTD expression involves a pool of AMPARs regulated by the NSF-GluR2 interaction. *Neuron*. 24:288–290.

Malenka, R. C., and R. A. Nicoll. 1999. Long-term potentiation—a decade of progress? *Science*. 285:1870–1874.

Malinow, R., H. Schulman, and R. W. Tsien. 1989. Inhibition of postsynaptic PKC or CaMKII blocks induction but not expression LTP. *Science*. 245:862–866.

Malinow, R., Z. F. Mainen, and Y. Hayashi. 2000. LTP mechanisms: from silence to four-lane traffic. *Curr. Opin. Neurobiol*. 10:352–357.

Mammen, A. L., K. Kameyama, K. W. Roche, and R. L. Huganir. 1997. Phosphorylation of the alpha-amino-3-hydroxy-5-methylisoxazole4-propionic acid receptor GluR1 subunit by calcium/calmodulin-dependent kinase II. *J. Biol. Chem*. 272:32528–32533.

McAllister, A. K., and C. F. Stevens. 2000. Nonsaturation of AMPA and NMDA receptors at hippocampal synapses. *Proc. Natl. Acad. Sci. USA*. 97:6173–6178.

McGlade-McCulloh, E., H. Yamamoto, S. E. Tan, D. A. Brickey, and T. R. Soderling. 1993. Phosphorylation and regulation of glutamate receptors by calcium/calmodulin-dependent protein kinase II. *Nature*. 362: 640–642.

Mosbacher, J., R. Schoepfer, H. Monyer, N. Burnashev, P. H. Seeburg, and J. P. Ruppersberg. 1994. A molecular determinant for submillisecond desensitization in glutamate receptors. *Science*. 266:1059–1062.

Partin, K. M., M. W. Fleck, and M. L. Mayer. 1996. AMPA receptor flip/flop mutants affecting deactivation, desensitization, and modulation by cyclothiazide, aniracetam, and thiocyanate. *J. Neurosci*. 16:6634–6647.

Poncer, J. C., J. A. Esteban, and R. Malinow. 2002. Multiple mechanisms for the potentiation of AMPA receptor-mediated transmission by alpha-Ca2+/Calmodulin-dependent protein kinase II. *J. Neurosci*. 22:4406–4411.

Rosenmund, C., Y. Stern-Bach, and C. F. Stevens. 1998. The tetrameric structure of a glutamate receptor channel. *Science*. 280:1596–1599.

Sheng, M., and S. H. Lee. 2001. AMPA receptor trafficking and the control of synaptic transmission. *Cell*. 105:825–828.

Sigworth, F. J. 1980. The conductance of sodium channels under conditions of reduced current at the node of Ranvier. *J. Physiol. (Lond.)*. 307:131–142.

Silva, A. J., C. F. Stevens, S. Tonegawa, and Y. Wang. 1992. Deficient hippocampal long-term potentiation in alpha-calcium-calmodulin kinase II mutant mice. *Science*. 257:201–206.

Smith, T. C., L. Y. Wang, and J. R. Howe. 2000. Heterogeneous conductance levels of native AMPA receptors. *J. Neurosci*. 20:2073–2085.

Smith, T. C., and J. R. Howe. 2000. Concentration-dependent substrate behavior of native AMPA receptors. *Nat. Neurosci*. 3:992–997.

Soderling, T. R., and V. A. Derkach. 2000. Postsynaptic protein phosphorylation and LTP. *Trends Neurosci*. 23:75–80.

Swanson, G. T., S. K. Kamboj, and S. G. Cull-Candy. 1997. Single-channel properties of recombinant AMPA receptors depend on RNA editing, splice variation, and subunit composition. *J. Neurosci*. 17:58–69.

Swope, S. L., S. I. Moss, L. A. Raymond, and R. L. Huganir. 1999. Regulation of ligand-gated ion channels by protein phosphorylation. *Adv. Second Messenger Phosphoprotein Res*. 33:49–78.

Traynelis, S. F., R. A. Silver, and S. G. Cull-Candy. 1993. Estimated conductance of glutamate receptor channels activated during EPSCs at the cerebellar mossy fiber-granule cell synapse. *Neuron*. 11:279–289.

Yoshimura, Y., C. Aoi, and T. Yamauchi. 2000. Investigation of protein substrates of Ca(2+)/calmodulin-dependent protein kinase II translocated to the postsynaptic density. *Brain Res. Mol. Brain Res*. 81: 118–128.